Probing neutrino magnetic moment and unparticle interactions with Borexino

Daniele Montanino,[1] Marco Picariello,[1] and João Pulido[2]

[1]*Dipartimento di Fisica, Università del Salento and Sezione INFN di Lecce, Via Arnesano, I-73100 Lecce, Italy*

[2]*Departamento de Fisica, Instituto Superior Tecnico, Centro de Fisica Teorica das Particulas, 1049-001 Lisboa, Portugal*

(Received 19 March 2008; revised manuscript received 9 April 2008; published 28 May 2008)

We discuss the limits on the neutrino magnetic moment and hypothetical interactions with a hidden unparticle sector, coming from the first neutrino data release of the Borexino experiment. The observed spectrum in Borexino depends weakly on the solar model used in the analysis, since most of the signal comes from the monoenergetic ^{7}Be neutrinos. This fact allows us to calibrate the $\nu - e$ scattering cross section through the spectral shape. In this way, we have derived a limit on the magnetic moment for the neutrinos coming from the Sun (in which a ν_μ and ν_τ component is present): $\mu_\nu \leq 8.4 \times 10^{-11} \mu_B$ (90% CL) which is comparable with those obtained from low-energy reactor experiments. Moreover, we improve the previous upper limit on magnetic moment of the ν_τ by 3 orders of magnitude and the limit on the coupling constant of the neutrino with a hidden unparticle sector.

DOI: 10.1103/PhysRevD.77.093011 PACS numbers: 26.65.+t, 13.15.+g, 14.60.Lm, 14.60.St

I. INTRODUCTION

The present experimental world neutrino data (apart the LSND experiment, which was not confirmed by the recent MiniBooNE result) provide a robust interpretation in terms of a three active neutrino oscillation scenario (for a recent review, see e.g. [1]). In particular, solar neutrinos together with KamLAND data, can be explained in a simplified two-neutrino framework (in the limit of a vanishing θ_{13}) with [2]

$$\begin{aligned} \Delta m^2_{12} &= (7.58 \pm^{0.21}_{0.20}) \times 10^{-5}\ \text{eV}^2, \\ \tan^2\theta_{12} &= 0.56 \pm^{0.14}_{0.09}. \end{aligned} \tag{1}$$

However, there is still room for subleading nonstandard neutrino interactions in the interpretation of data. For example, an evidence for time modulation of the oscillation probability in the solar neutrinos could be explained in terms of a nonzero magnetic moment, which could induce transitions among active and sterile neutrinos [3].

Recently, the Borexino collaboration has released the first data relative to about three months of data taking [4]. In this experiment, solar neutrinos (mainly, those coming from the ^{7}Be source) are detected through $\nu - e$ scattering and the recoil electron energy is measured through a scintillation technique. The observed event rate is essentially consistent with the one predicted by the standard solar model [5] and the oscillation hypothesis. However, since the main source observed in Borexino is the monoenergetic 863 keV ^{7}Be source, a precise calibration of the differential $d\sigma/dT_e(E_\nu, T_e)$ cross section (where E_ν is the incident neutrino energy and T_e the recoil electron kinetic energy) is possible through a spectral shape analysis. For example, neutrino electromagnetic form factors would influence the scattering cross section [6]. In particular, a nonzero neutrino magnetic moment introduces a term which grows with the inverse of both the energy of the incident neutrino and with that of the recoil electron. For this reason, a low-energy experiment (such as Borexino) is in a favorable situation.

Although the limits obtained are still weaker than those obtained by a direct measurement of the $\bar{\nu}_e - e$ scattering in reactor experiments [7,8] (and those that could be obtained by Borexino itself from a calibration experiment with an external source of neutrinos or antineutrinos [9]), we should stress that these are short baseline experiments, and they measure the magnetic moment of the $\bar{\nu}_e$ component. Instead, solar neutrinos embed also a component of ν_μ and ν_τ, for which the limits are much weaker [10,11]. SuperKamiokande data were used in the past to study the neutrino magnetic moment [12–16], but since this experiment observes the continuous ^{8}B source, it is difficult to disentangle the effects of a spectral distortion due to nonstandard interactions and those due to the oscillation mechanism. In the past, the Borexino collaboration tried to put a limit on μ_ν using the prototype of the Borexino detector (the Counting Test Facility, CTF) [17]. However, at that time, due to the smallness of the CTF, no solar neutrinos were observed and a limit was established assuming the theoretical SSM neutrino flux.

Concerning other nonstandard interactions, the possibility of a conformal hidden sector, called the "unparticle sector," which couples to the various gauge and matter fields of the SM through nonrenormalizable interactions, has been recently proposed [18]. The unparticle sector is assumed to have a nontrivial infrared fixed point, $\Lambda_{\mathcal{U}}$, below which the sector has a scale invariance and the hidden operators become an effective unparticle operator with nonintegral scaling dimension d. Limits from low-

energy neutrino-electron scattering in the unparticle physics framework have been recently obtained in [19]. We will show that the limits coming from Borexino are stronger.

The plan of the paper is the following. In Sec. II we review the contribution to the cross section due to the neutrino magnetic moment or the coupling with the unparticle sector; in Sec. III we describe briefly the experimental input; in Sec. IV we describe our analysis technique; in Sec. V we derive the upper bounds on the neutrino magnetic moment from SK and Borexino experiments, emphasizing the fact that the former is quite sensitive to the solar model assumed while the latter is independent; finally, in Sec. VI we draw our conclusions.

II. ELECTRON-NEUTRINO CROSS SECTION

A. Neutrino magnetic moment

For a neutrino with flavor a, the scattering process standard differential $\nu_a - e$ cross section as a function of the incident neutrino energy E_ν and of the recoil electron kinetic energy T_e, is given by [20][1]

$$\frac{d\sigma_a^{\rm std}}{dT_e}(E_\nu, T_e) = \frac{\sigma_0}{m_e}\Big[(g_V^a + g_A^a)^2 + (g_V^a - g_A^a)^2\Big(1 - \frac{T_e}{E_\nu}\Big)^2 - ((g_V^a)^2 - (g_A^a)^2)\frac{m_e T_e}{E_\nu^2}\Big], \quad (2)$$

with $\sigma_0 = G_F^2 m_e^2/(2\pi)$. For μ and τ neutrinos, where only neutral current interactions are possible, the standard model of electroweak interactions provides $g_V^{\mu,\tau} = 2\sin^2\theta_W - \frac{1}{2}$ and $g_A^{\mu,\tau} = -1/2$, with $\sin^2\theta_W = 0.23122$ [10]. For electron neutrinos, where also charge current interactions are possible, we have $g_{V,A}^e \to g_{V,A}^{\mu,\tau} + 1$.

Besides standard interactions, neutrinos can couple with photons through a possible magnetic dipole and/or charge radius. The effective low-energy $\nu - \gamma$ interaction vertex is [6]

$$(\Gamma^\rho_{\nu-\gamma})_{ab} = \bar\nu_b\Big[\frac{\langle r_\nu^2\rangle_{ab}}{6}q^2\gamma^\rho - \frac{1}{2m_e}(\mu_{ab} + d_{ab}\gamma^5)\sigma^{\rho\lambda}q_\lambda\Big]\nu_a, \quad (3)$$

where $\langle r_\nu^2\rangle_{ab}$ is the charge radius and μ_{ab} and d_{ab} are the neutrino magnetic and electric dipole moments, respectively. Since for ultrarelativistic neutrinos it is not possible to distinguish between the two dipole moments, for simplicity we consider only magnetic moments. For an individual incoming neutrino with flavor a, since the outgoing neutrino flavor is in general not observable, the only phenomenologically relevant parameter is a combination of the magnetic moment matrix μ_{ab}:

$$\mu_a = \sqrt{\sum_b |\mu_{ab}|^2}. \quad (4)$$

For Dirac neutrinos μ_{ab} is a generic complex matrix and involves transitions among left and right (sterile) states. Conversely, for Majorana neutrinos the transitions are among neutrino and antineutrino states of different flavours. In this case the matrix μ_{ab} is antisymmetric (and, in particular, $\mu_{aa} = 0$).

Actually, the charge radius could be absorbed in a redefinition of the g_V's:

$$g_V^a \to g_V^a + \frac{2M_W^2}{3}\langle r_\nu^2\rangle_a \sin^2\theta_W. \quad (5)$$

However, as we will comment later, Borexino is largely insensitive to variations on the axial and vector couplings g_V^a and g_A^a within the limits coming from present phenomenology [22]. For this reason, we limit our analysis to the magnetic moment assuming standard values for g_V^a and g_A^a.

Since the neutrino flavor composition in the experiments considered here depends on the energy range of each experiment, the bounds we derive in this work are actually applicable to an effective neutrino magnetic moment, which is a linear combination of the individual flavor magnetic moments whose coefficients depend, as will be seen later, on the weighted average survival probability for each experiment.

Robust cosmological arguments show that μ_ν should be smaller than 10^{-8} Bohr magnetons, μ_B, [23], although other astrophysical arguments largely override this bound (see, e.g., [24] and reference therein). However, such arguments are model dependent and thus less reliable. The strongest direct bounds on the $\bar\nu_e$ come from the TEXONO experiment [7], i.e., $\mu_e < 0.74 \times 10^{-10}\mu_B$ and, more recently, from the GEMMA experiment, i.e., $\mu_e < 0.58 \times 10^{-10}\mu_B$ at 90% C.L. [8]. However the limits for the $\mu_{\mu,\tau}$ are much weaker ($\mu_\mu < 6.8 \times 10^{-10}\mu_B$ [25], $\mu_\tau < 3900 \times 10^{-10}\mu_B$ [26]).

The contribution to the $\nu_a - e$ cross section due to the neutrino magnetic moment interaction is given by [6]

$$\mu_a^2\frac{d\sigma^\mu}{dT_e}(E_\nu, T_e) = \frac{\pi\alpha_{\rm e.m.}^2}{m_e^2}\Big(\frac{\mu_a}{\mu_B}\Big)^2\Big(\frac{1}{T_e} - \frac{1}{E_\nu}\Big), \quad (6)$$

where we have explicitly factorized out the μ_a dependence from the expression of the cross section. A comment is in order. In principle an interference term between the magnetic moment and the weak interaction is possible. However, this interference term vanishes if the neutrinos are longitudinally polarized and the electrons are unpolarized. If neutrinos cross a strong magnetic field (such as the solar one) they can acquire a transverse polarization due to the precession. In this case an interference effect could contribute to the cross section [6]. Here we neglect this effect since the first Borexino data was taken in a period of low magnetic field activity.

[1] In this work for completeness we have also included the 1-loop corrections to this formula [21]. However, the effect of such corrections is negligible.

B. Coupling with unparticles

Recently, a scale invariant ("unparticle") sector which decouples at high energy was proposed in [18]. Leptons can couple, for example, with a scalar unparticle sector [18,27,28] through the Lagrangian[2]

$$\mathcal{L}_{\mathcal{U}} = \lambda_e \frac{1}{\Lambda_{\mathcal{U}}^{d-1}} \bar{e} \hat{O}_{\mathcal{U}} e + \sum_{a,b} \lambda_\nu^{ab} \frac{1}{\Lambda_{\mathcal{U}}^{d-1}} \bar{\nu}_a \hat{O}_{\mathcal{U}} \nu_b + \text{H.c.}, \tag{7}$$

where d is the nonintegral scaling mass dimension of the unparticle operator, $\Lambda_{\mathcal{U}}$ is a typical scale of the unparticles physics and it can be assumed $\sim O(\text{TeV})$, $\hat{O}_{\mathcal{U}}$ is the unparticle operator, and the λ's are the coupling constants of the leptons to the unparticle sector (possible flavor changing interactions $\nu_a \to \nu_b$ have been also taken into account). The contribution to the scattering amplitude for elastic $\bar{\nu}_a - e$ scattering from the exchange with a scalar unparticle is [19]

$$\mathcal{M}^{ab} = \lambda_\nu^{ab} \lambda_e \frac{\mathcal{F}(d)}{\Lambda_{\mathcal{U}}^{2d-2}} \Big[\bar{\nu}_b(k_f) \nu_a(k_i) \Big] \frac{1}{(-q^2)^{2-d}} \times \Big[\bar{e}(p_f) e(p_i) \Big], \tag{8}$$

where $q = k_f - k_i$ and

$$\mathcal{F}(d) = \frac{8\pi^{5/2}}{(2\pi)^{2d} \sin(\pi d)} \frac{\Gamma(d + 1/2)}{\Gamma(d-1)\Gamma(2d)}. \tag{9}$$

From this amplitude, the contribution to the $\nu_a - e$ cross section can be calculated[3]:

$$\lambda_a^2 \frac{d\sigma^{\mathcal{U}}}{dT_e}(E_\nu, T_e) = \lambda_a^2 \frac{2^{2d-7} \mathcal{F}^2(d)}{\pi E_\nu^2 \Lambda_{\mathcal{U}}^{4d-4}} (m_e T_e)^{2d-3} (T_e + 2m_e), \tag{10}$$

and we have conveniently defined

$$\lambda_a = \sqrt{\sum_b (|\lambda_\nu^{ab}| \lambda_e)^2}. \tag{11}$$

As in the case of magnetic moment, the final state will be a sterile right state or an antineutrino state depending on the Dirac or Majorana nature of the neutrinos. Notice that for $d < 3/2$ the cross section diverges for low T_e, thus low-energy experiments are most sensitive to the unparticles. Notice that for $d = 1$ we have the same T_e^{-1} dependence as in the case of the magnetic moment.

[2]In general, the coupling with a vector or tensor unparticle is also possible. Here, for simplicity, we consider only the scalar case.

[3]One can easily check that for almost massless neutrinos the interference term with the standard amplitude is negligible.

III. THE EXPERIMENTAL INPUT

The Borexino experiment at the Gran Sasso underground laboratory is designed to study mainly the 863 keV monoenergetic ^{7}Be solar neutrinos, through a real-time and low-background detector. A detailed description of the experimental apparatus and its ancillary plants can be found in [29]. Briefly, Borexino consists of 300 tons of a high purity liquid organic scintillator (pseudocumene, C_9H_{12}, $\rho = 0.88$ g/cm^3) doped with PPO at 1.5 g/l. The scintillator mixture is contained inside a thin nylon sphere (8.5 m in diameter). This volume is viewed by 2212 8" photomultipliers (PMTs) installed on a stainless steel sphere of 13.7 m in diameter. The scintillator is shielded against background from PMTs and other external sources by a 2.5 m buffer of pseudocumene, an outer nylon vessel and 2 m of high purity water. For solar neutrinos search a fiducial volume of 100 tons is selected offline. In Borexino solar neutrinos are detected through the scattering reaction $\nu + e \to \nu + e$. The recoil electron energy is converted into light inside the scintillator. The intrinsic ^{14}C contamination[4] and finite energy resolution set the detection threshold at about 200 keV. In Borexino no directionality is possible to search for neutrino interactions and it is not possible to distinguish on an event-by-event basis between neutrino processes and β/γ backgrounds. Therefore, the radiopurity of the scintillator is a fundamental experimental issue. The first results [4] have shown that the radiopurity achieved is beyond the expectations and this allows to extend the research program as we attempt to do in this work.

The data taking started in May 2007. The collaboration released the first data in August 2007 [4]. The observed flux of ^{7}Be neutrinos is (within the errors) consistent with the standard solar model prediction in the hypothesis of Mikheyeev-Smirnov-Wolfenstain oscillations, i.e., $47 \pm 7(\text{stat}) \pm 12(\text{sys})$ counts per day (cpd) in 100 tons for the ^{7}Be (863 keV) neutrinos, against a theoretical value of 49 ± 4 cpd's. The collaboration has also produced a spectrum of the observed events with the visible electron energy K_e in the range $270 \le K_e \le 800$ keV. This spectrum is shown in Fig. 6 of [4], in which the number of events per day and per 100 tons of scintillator are shown in 53 bins of energy (we show our equivalent plot in Fig. 1). The collaboration quote a 15% uncorrelated error for each bin. However, since there are also bins with less than three events, the mere statistical error for these bins would be greater than 15%. For this reason we prefer to be conservative and sum in quadrature the 15% error quoted by the collaboration to the statistical error $N_i^{-1/2}$, where N_i is the number of events in each bin. In the majority of bins, where $N_i \gg 3$, the statistical error is negligible and the uncorrelated error is just that quoted by the collaboration. The

[4]The ^{14}C have a β decay with an endpoint energy of 156 keV.

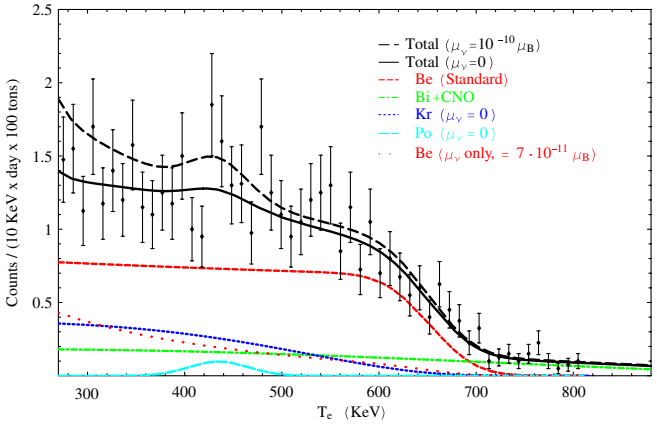

FIG. 1 (color online). The "best fit" spectrum with zero (black solid line) and nonzero (black dashed line) magnetic moment. The contributions of the ^{7}Be source (red medium-dashed line) and those from the CNO + ^{210}Bi (green dotted-dashed line), ^{85}Kr (blue dotted line), and ^{210}Po (light blue log-dashed line) in the case $\mu_\nu = 0$ are also shown. The number of counts per day in the "best fit" ($\mu_\nu = 0$) case in the whole energy range are 49 for the ^{7}Be, 12 for the CNO + ^{210}Bi, 18 for the ^{85}Kr, and 1 for the ^{210}Po source. For illustration, we also show the contribution coming from the magnetic moment only for $\mu_\nu = 7 \times 10^{-11}\mu_B$ (red dotted line).

main source of correlated error comes from the determination of the fiducial mass. The collaboration quotes a 25% error equally correlated among all bins.

From [4] we know that the measured light yield is about 500 photoelectrons/MeV. The light yield affects the energy resolution of the detector and at a first approximation we can assume a Gaussian energy smearing with $\sigma = \sqrt{T_e/500}$. We notice that this assumption does not work well in the low-energy regime (mainly below 200 keV) where nonlinear effects due to quenching take place. In the energy range we are considering, namely [270, 800] keV this effect is expected to be on the order of a few %'s. With the above assumption the resolution function for the detection of solar neutrinos is thus

$$\mathcal{R}(K_e, T_e) = \frac{1}{\sqrt{2\pi}\sigma} \exp\left[-\frac{(K_e - T_e)^2}{2\sigma^2}\right], \qquad (12)$$

where T_e is the *real* kinetic electron energy, K_e is the visible (measured) one, and $\sigma = 4.47\%\sqrt{T_e}$.

The main sources of background in the detector come from the decay of contaminants contained in the scintillator (being the cosmogenic contribution almost completely rejected by muon vetoing and other techniques with the exception of ^{11}C which, however, could dominate the spectrum above 1 MeV). Internal background is due to the β decays of ^{210}Bi and ^{85}Kr and the α decay of ^{210}Po as reported in [4]. The former background is enormously reduced by α/β pulse shape discrimination (PSD). However, the rejection efficiency of the PSD is not 100% and may change with the energy. In our analysis we adopt the same assumption used in [4] and take into account a possible small residual of α-like events in the β-like/neutrino events spectrum by means of a Gaussian peaked around 410 KeV:

$$\tilde{S}_\alpha(K_e) = \mathcal{N}_{^{210}\mathrm{Po}} \cdot \mathcal{R}(K_e, 410\ \mathrm{KeV}). \qquad (13)$$

Here $\mathcal{N}_{^{210}\mathrm{Po}}$ is the unknown normalization to the spectrum that should be determined by the fit.

As pointed out above, β decays cannot be rejected. They contribute to the total spectrum through the

$$S_\beta(T_e) = \sum_B \mathcal{N}_B \left(1 - \frac{T_e}{Q_B}\right)^2 \frac{E_e p_e}{Q_B^2} F_B(T_e), \qquad (14)$$

where $B \in \{^{210}\mathrm{Bi}, ^{85}\mathrm{Kr}\}$, $E_e = T_e + m_e$ and $p_e = \sqrt{2m_e T_e + T_e^2}$ are the total electron energy and momentum, and the Fermi correction F_B is given by [30]

$$F_B(T_e) = 2(1+\gamma_0)(2Rp_e)^{2\gamma_0-2} e^{\pi\nu} \frac{|\Gamma(\gamma_0 + i\nu)|^2}{\Gamma(2\gamma_0+1)^2}, \qquad (15)$$

where $R = 0.426A^{1/3}\alpha_{\mathrm{e.m.}}/m_e$ is approximately the radius of the nucleus and, in turn,

$$\nu(T_e, Z) = \alpha_{\mathrm{e.m.}} Z E_e / p_e, \qquad \gamma_0 = \sqrt{1 - \alpha_{\mathrm{e.m.}}^2 Z^2},$$

where A and Z are the atomic number and charge of the parent nucleus, respectively. The Q values for the two β sources are 1162.1 KeV for the ^{210}Bi and 687.1 KeV for the ^{85}Kr. Moreover, since the β decay of the ^{85}Kr is forbidden, the spectrum should be corrected by the multiplicative factor $p_e^2/Q^2 + (1 - T_e/Q^2)^2$ [30]. Of course the observed β spectrum is the convolution of the true spectrum with the resolution function.

IV. ANALYSIS

The observed total spectrum in Borexino is given by

$$S(K_e) = \sum_s \mathcal{N}_s \Phi_s \int dE_\nu \varphi_s(E_\nu) \sum_a \frac{d\tilde{\sigma}_a}{dT_e}(E_\nu, K_e) \cdot P_{ea}(E_\nu) + \tilde{S}_\alpha(K_e) + \tilde{S}_\beta(K_e), \qquad (16)$$

where $s \in \{\mathrm{pp}, \mathrm{pep}, ^7\mathrm{Be}, ^{16}\mathrm{O}, ^{14}\mathrm{N}\}$ are the solar sources (the contribution from ^{8}B and hep neutrinos is negligible) with their (normalized) spectra φ_s and standard solar model flux Φ_s (in particular, we have used the AGS05 fluxes, see Table 6 of [5]), $P_{ea}(E_\nu)$ is the oscillation probability $P(\nu_e \to \nu_a)$, and $\mathcal{N}_s$ are normalization factors (with the constraint $\mathcal{N}_s \geq 0$); the "tilde" means that the cross sections/background spectra have been convoluted with the resolution function. In practice the CNO sources (i.e., the ^{16}O, ^{14}N) give a small contribution to the spectrum. Moreover, their spectra are almost indistinguishable among them and from those of the ^{210}Bi background. Since we do not expect a strong spectral distortion from oscil-

lations, following the Borexino paper, we have embedded the CNO contribution into the ^{210}Bi spectrum.

For ^{7}Be and pep neutrinos the spectrum is almost monoenergetic apart a few keV broadening due mainly to collision and thermal effects [31]. In the energy range explored by the experiment the only contribution to the spectrum comes from the 863 keV ^{7}Be line, the contribution from the other line (385 KeV) being well below the threshold. In our analysis we fix only the pp and pep neutrinos at their standard solar model value (i.e., we force $\mathcal{N}_{\mathrm{pp,pep}} = 1$) [5], as their sources are affected by a very low theoretical uncertainty ($\sim 1\%$–2%). All the other solar fluxes, the background normalizations and, of course, the nonstandard parameters, are taken as free variables in the fit.

Regarding the oscillation probability, we have used the standard Mikheyev-Smirnov-Wolfenstein (MSW) probability with the oscillation parameters defined in Eq. (1).[5] We do not fit the mass-mixing parameters with Borexino data since it is not the goal of this work. A comment is in order. In principle when nonstandard interactions are present, also the oscillation probability could be affected by new interactions. In particular, the neutrino magnetic moment can induce resonant spin-flip precession [33] (for a recent review, see also [34], Sec. 13.1 and reference therein). Anyway, barring oscillations into sterile neutrinos, any change in the probability would reflect only in a very small change of the spectral shape (since it is determined mainly by the ^{7}Be line), while the overall normalization is left free.[6] For this reason, the precise choice of the probability is not critical to our scope, provided that: (1) no active-sterile oscillations are allowed and (2) no dramatic spectral distortion in the CNO spectra are expected.

We now have all the ingredients to calculate the χ^2[7]:

$$\chi^2 = \sum_{ij} (N_i^{\mathrm{Th}} - N_i^{\mathrm{Exp}})(\sigma^{-2})_{ij}(N_j^{\mathrm{Th}} - N_j^{\mathrm{Exp}}), \tag{17}$$

where N_i^{Exp} (N_i^{Th}) is the experimental (theoretical) number of events in the ith bin, and, as explained in the previous section, the matrix σ_{ij}^2 is calculated as

$$\sigma_{ij}^2 = [N_i^{\mathrm{Exp}} + (0.15 N_i^{\mathrm{Exp}})^2]\delta_{ij} + (0.25 N_i^{\mathrm{Exp}}) \cdot (0.25 N_j^{\mathrm{Exp}}). \tag{18}$$

Since all the unknown parameters appear linearly in the calculation of N_i^{Th}, the χ^2 minimization is straightforward. Defining

$$F_i^k = \frac{\partial N_i^{\mathrm{Th}}}{\partial \mathcal{N}_k} \tag{19}$$

(with $k \in \{\mathrm{pp}, \mathrm{pep}, {}^{7}\mathrm{Be}, \mathrm{CNO} + {}^{210}\mathrm{Bi}, {}^{85}\mathrm{Kr}, {}^{210}\mathrm{Po}\}$), it is easy to show that

$$\mathcal{N}_k = \sum_i [(\mathbf{F}\sigma^{-2}\mathbf{F}^T)^{-1}\mathbf{F}\sigma^{-2}]_{ki}\left(N_i^{\mathrm{Exp}} - \sum_{s\in\{\mathrm{pp,pep}\}} \mathcal{N}_s F_i^s\right), \tag{20}$$

where the pp and pep sources are fixed and not fitted. In any case, negative $\mathcal{N}_k$'s are not allowed.

The "best fit" spectrum with standard interactions only is shown in Fig. 1, which is similar to Fig. 6 of [4], with the black solid line. (In the figure is shown also the spectrum with a nonzero magnetic moment with the black dashed line). For comparison, we also report the number of events per day in the full recoil energy range for each source for 100 Tons of scintillator in our "best fit" case: 49 for the ^{7}Be, 12 for the CNO + ^{210}Bi, 18 for the ^{85}Kr, and 1 for the ^{210}Po.

The value of χ^2_{min} is 37.6, is slightly lower than the one obtained by the collaboration ($\chi^2_{\mathrm{min}} = 41.9$), due to different assumptions in the two analyses. In the same figure the various contributions (apart those from pp and pep neutrinos which are very small) are also shown. The main contributions to the spectrum come from the CNO + ^{210}Bi, ^{85}Kr, and ^{210}Po. Among these, only the first could be slightly affected by the functional form of $P_{ea}(E_\nu)$. We see also that this contribution as almost flat, while those from ^{210}Po is a peculiar "bump." The main contribution for the spectral distortion at low energies (thus mimicking those coming from nonstandard interactions) comes from the ^{85}Kr background. As we will discuss later, this background is the main limitation to the measure.

V. LIMITS ON THE NONSTANDARD INTERACTIONS

Introducing the nonstandard interactions, we see that the main contribution to the spectral distortion comes from ^{7}Be neutrinos. In particular, we see that, if only ^{7}Be neutrinos are taken into account, the contribution to the spectrum coming from the nonstandard interactions is

$$\delta S(K_e) = \xi_{\mathrm{eff}}^2 \cdot \frac{d\tilde{\sigma}^{\mathrm{nonstd}}}{dK_e}(E_\nu, T_e), \tag{21}$$

where $\xi \equiv \mu_\nu$, λ_ν and $d\tilde{\sigma}^{\mathrm{non,std}}/dK_e$ is the nonstandard contribution given by Eqs. (6) or (10), after the proper convolution with the resolution function. The label "eff" means that we must consider an effective coupling, given

[5] We have used the approximate formulae for calculating the P_{ee} survival probability already averaged over the production zone given in [32].

[6] Moreover, to simplify our analysis, we do not allow any $\nu \leftrightarrow \bar{\nu}$ transitions so that $\bar{\nu}$'s are absent in the flux.

[7] In the presence of bins with zero or few events the χ^2 function should in principle be corrected as prescribed in [10]. However, since the low statistic bins are less relevant for the analysis, we prefer to use the standard χ^2. In this way the unknown parameters can be extracted analytically.

by

$$\xi^2_{\rm eff} = \sum_a P_{ea}(E^0_\nu) \cdot \xi^2_a, \tag{22}$$

where $E^0_\nu = 863$ keV is the energy of the ^{7}Be neutrinos. Because of the unitarity of the probability, this is also equivalent to introducing an equal magnetic moment (μ_ν) or unparticle coupling (λ_ν) to all flavors. Since also nonmonochromatic sources contribute to the spectra, for simplicity we stick into this simplified hypothesis of equal nonstandard parameters. However, since the final result of the analysis does not depend critically on the functional form of P_{ea}, the limits on μ_ν and λ_ν are practically a limit on $\mu_{\rm eff}$ and $\lambda_{\rm eff}$.

In particular, if we trust that the oscillation is simply given by the MSW effect with small θ_{13}, we have that $\mu^2_{\rm eff}$ and $\lambda^2_{\rm eff}$ are given by

$$\mu^2_{\rm eff} = P^{2\nu}(E^0_\nu) \cdot \mu^2_e + [1 - P^{2\nu}(E^0_\nu)] \times (\cos^2\theta_{23} \cdot \mu^2_\mu + \sin^2\theta_{23} \cdot \mu^2_\tau) \tag{23}$$

(and, of course, a similar expression holds for $\lambda_{\rm eff}$). In principle, in the previous equation interference terms among oscillation amplitudes can be present. However, with the oscillation parameter given in Eq. (1) these terms average out and can be safely neglected [6,15].[8] In Eq. (23) $P^{2\nu}(E^0_\nu)$ is the two-neutrino $P(\nu_e \to \nu_e)$ standard MSW probability and $\sin^2\theta_{23} = 0.38$–0.63 (2σ) from recent atmospheric and accelerator (K2K and MINOS) analysis [1]. Moreover, for low-energy neutrinos we have also that with good approximation $P^{2\nu} \simeq \cos^2\theta_{12} \simeq 1/2$.

A. Limits on the magnetic moment

We start by deriving the upper bound on the effective magnetic moment from the SuperKamiokande (SK) experiment. To this end, the flux measured by SK is

$$\Phi_{\rm SK} = \Phi_{\rm 8B} \frac{\int dE_\nu \varphi_{\rm 8B}(E_\nu) \sum_a P_{ea}(E_\nu)[\sigma^{\rm std}_a(E_\nu) + \mu^2_\nu \sigma^\mu(E_\nu)]}{\int dE_\nu \varphi_{\rm 8B}(E_\nu) \sum_a P_{ea}(E_\nu)\sigma^{\rm std}_e(E_\nu)}, \tag{24}$$

where $\sigma^{\rm std}_a$ and σ^μ are the total (standard and nonstandard) cross sections in the SK energy range. In this case it is not possible to define an effective magnetic moment as in Eq. (23), so, for simplicity, we have assumed an equal μ_ν for all flavors.

From Eq. (24) we realize that the bound on μ_ν depends on the total ^{8}B flux (and hence is solar model dependent). For example, using the AGS05 model [5] where $\Phi_{\rm 8B} = 4.51 \times 10^6 \times (1 \pm 0.12)$ cm^{-2} s^{-1} with the SK measured rate $R_{\rm SK} = [2.35 \pm 0.02({\rm stat}) \pm 0.08({\rm sys})] \times 10^6$ cm^{-2} s^{-1} we obtain $\mu_\nu < 2.1 \times 10^{-10}\mu_B$ (90% CL). On the other hand for the GS98 [5] model with the higher ^{8}B flux $\Phi_{\rm 8B} = 5.69 \times 10^6 \times (1 \pm 0.16)$ cm^{-2} s^{-1} we obtain a stronger bound, $\mu_\nu < 1.3 \times 10^{-10}\mu_B$ (90% CL), which is more in agreement with the bound obtained by the spectral analysis done by the SK collaboration [16].

As far as Borexino is concerned, the corresponding upper bound on the neutrino magnetic moment is not dependent on the standard solar model assumed. In fact the ^{7}Be normalization is extracted from the experimental data. In order to show the effect of the magnetic moment, in Fig. 1 in the black dashed line we plot also the theoretical spectrum for $\mu_\nu = 10^{-10}\mu_B$ (which is well beyond the 90% limit). From the plot we see that (as expected) the spectrum grows at low energies. This behavior, as we discuss later, can be also mimicked by the ^{85}Kr background.

In Fig. 2 we show the χ^2 as function of the neutrino magnetic moment where all the free fluxes and backgrounds have been marginalized. We see that the 90% C.L. limit on the magnetic moment is $\mu_\nu \leq 8.4 \times 10^{-11}\mu_B$.[9] We have also tried to fit the neutrino charge radius and more in general the neutrino vector and axial couplings g_V and g_A, as proposed in [35]. Unfortunately the limits obtained with Borexino are far from being competitive from those obtained by other experiments [22]. However, we have verified that varying g_V and g_A inside the allowed region(s) in Fig. 2 of [22] our limit on μ_ν does not vary appreciably.

Although this limit is less competitive than those obtained from reactor experiments like in GEMMA ($\mu_e < 5.8 \times 10^{-11}\mu_B$ at 90% C.L., [8]), we should bear in mind that reactor experiments are short baseline. For this reason, the limits obtained in these experiments are essentially bounds on the μ_e component. Instead, the limits coming from solar neutrinos can be translated into limits for μ_μ and μ_τ. In particular, we have seen that for Borexino the limit on μ_ν is practically a limit on $\mu_{\rm eff}$. Using Eq. (23) and $P^{2\nu} \simeq 1/2$ we obtain a conservative limit on μ_τ (obtained in the worst case $\mu_e = \mu_\mu = 0$ and $\sin^2\theta_{12}$, $\cos^2\theta_{23}$ taken at their 2σ minimum allowed values):

[8]Note that our definition of μ_a is different from those used in Ref. [15].

[9]In [15] a perspective analysis of the Borexino experiment was performed. Although they obtained a more stringent limit on a combination of the Majorana magnetic transition moments, they assumed a fixed background. As we will see later, the main source of uncertainty comes from the lack of knowledge of the true number of background events.

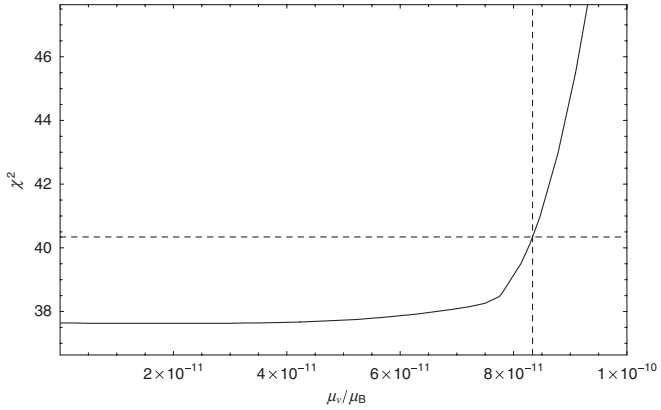

FIG. 2. The χ^2 as a function of the neutrino magnetic moment μ for standard axial and vectorial coupling. We also report the 90% C.L. ($\chi^2 - \chi^2_{\rm min} = 2.71$).

$$\mu_\tau \lesssim 1.9 \times 10^{-10} \mu_B, \tag{25}$$

which is 3 orders of magnitude stronger than those quoted by the Particle Data Group ($\mu_\tau < 3900 \times 10^{-10} \mu_B$ [10]). Equivalently, we get the limit

$$\mu_\mu \lesssim 1.5 \times 10^{-10} \mu_B. \tag{26}$$

The "plateau" in the χ^2 for $\mu_\nu \lesssim 0.85 \times 10^{-10} \mu_B$ is due to the partial compensation between the ^{85}Kr background and the magnetic moment contribution (we have also checked that the other normalization factors are almost insensitive to the value of μ_ν). In fact both the magnetic moment and the ^{85}Kr, have the same effect in the spectrum, i.e., to increase the slope at low energies. Increasing μ_ν the slope is kept almost constant if one simultaneously decreases the normalization of the ^{85}Kr background. For example, this can be also seen in Fig. 1 from the comparison between the red dotted line (which is the contribution of the magnetic moment to the electron spectrum due to ^{7}Be neutrinos, for $\mu_\nu = 7 \times 10^{-11} \mu_B$) and the blue dotted line (which is the contribution due to the ^{85}Kr in the absence of the magnetic moment). At $\mu_\nu \sim 0.85 \times 10^{-10} \mu_B$ the ^{85}Kr normalization vanishes and compensation is no longer possible. This can also be noticed in the abrupt discontinuity of the derivative of the χ^2.

The main limitation for the measure of μ_ν thus comes not from the limited statistics, but from the imprecise knowledge of the ^{85}Kr background. If in the future this background will be reduced by a purification campaign,[10] the limit on μ_ν would become much stronger. We also mention that by greatly improving the exposure, it might be possible to measure the ^{85}Kr contamination by means of correlated events as reported in [4]. Moreover, due to the Earth orbital eccentricity, the solar flux has periodical variations in one year, while the internal background is expected to be nearly constant in time. This means that a better limit on μ_ν could be obtained simply measuring the spectrum in different periods of the year.

TABLE I. Confrontation between our 90% C.L. limits on λ_ν with ^{7}Be unconstrained (third column) and fixed by the SSM fourth column for different value of d, with $\Lambda_{\mathcal{U}} = 1$ TeV. Also the limits obtained in [19] are shown (second column).

d	λ_ν (Table 1 of [19])	λ_ν (unconst. ^{7}Be)	λ_ν (SSM ^{7}Be)
1.01	3.5×10^{-6}	2.4×10^{-6}	1.8×10^{-6}
1.05	7.3×10^{-6}	4.8×10^{-6}	3.4×10^{-6}
1.1	1.9×10^{-5}	1.1×10^{-5}	0.8×10^{-5}
1.2	1.2×10^{-4}	0.6×10^{-4}	0.4×10^{-4}
1.3	7.2×10^{-4}	4×10^{-4}	2.9×10^{-4}
1.4	4.5×10^{-3}	1.8×10^{-3}	1×10^{-3}
1.5	2.7×10^{-2}	1×10^{-2}	0.5×10^{-2}
1.7	9.5×10^{-1}	2.4×10^{-1}	1×10^{-1}
1.9	24.5	4	2

B. Limits on unparticle coupling

We have done the analysis done in the previous section but using the unparticle cross section (10). All the considerations made in the previous section (in particular, the partial compensation between the ^{85}Kr background and the unparticle contribution) also apply in this case.

In Table I we show our limits on λ_ν as function of the dimension d. We fix the value of $\Lambda_{\mathcal{U}}$ to 1 TeV. Of course, if we choose a different value for $\Lambda_{\mathcal{U}}$, the limits on λ_ν should be rescaled according to Eq. (10). The values of d (first column) have been chosen in order to make a comparison with the limit obtained in Table I of [19]. In the third column we show our 90% C.L. limits on λ_ν obtained in the same way of the previous section, i.e., taking the ^{7}Be solar flux completely unconstrained. In the fourth column we show the same limit, but taking into account the 10.5% theoretical uncertainty on the ^{7}Be flux [5]. This is done simply by adding a penalty function to the χ^2

$$\chi^2 \to \chi^2 + \left(\frac{\mathcal{N}_{^7\rm Be} - 1}{\sigma_{^7\rm Be}}\right)^2. \tag{27}$$

As expected, in this case the bounds on λ_ν slightly improve.[11] In Fig. 3 we show also the 90% C.L. allowed zone in the plane (d, λ_ν) as from Ref. [19] (light gray), with unconstrained (dark gray) and constrained (black) ^{7}Be flux.

We see that our limits are even stronger than those obtained by Balantekin and Ozansoy [19]. We remark that the limits obtained in [19] are obtained using short baseline reactor data thus sensitive only to ν_e, while our result applies to the combination $\lambda_{\rm eff}$ in Eq. (22). Since $P_{ee} \sim 1/2$, sometimes our limits on λ_e alone can be

[10] We notice that due to the long mean-life of the ^{85}Kr, the fate and impact of this background are different than that of ^{210}Po.

[11] We have checked that in the case of the magnetic moment the improvement is negligible.

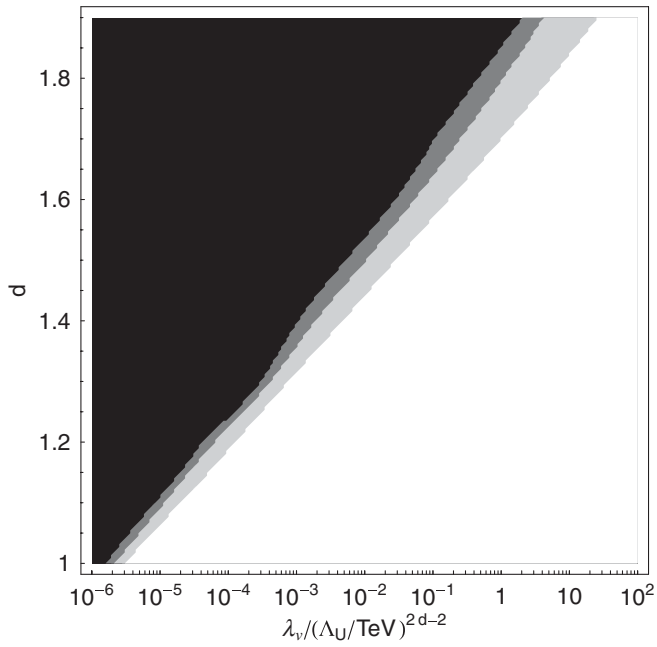

FIG. 3. The 90% C.L. allowed zone in the plane (d, λ_ν) (for $\Lambda_\mathcal{U} = 1$ TeV) as from Ref. [19] (light gray), with unconstrained ^{7}Be flux (dark gray) and with the ^{7}Be flux fixed by the standard solar model. See the text for more details.

weaker than those in [19]. However, combining our limits on λ_{eff} with those on λ_e in [19] we can obtain for the first time bounds on the coupling constants λ_μ and λ_τ in accordance with Eq. (23).

A comment is in order. In principle, unparticle interactions could affect also the production and propagation of neutrinos [36]. However, we have already stressed that the major contribution of the solar flux comes from the ^{7}Be monoenergetic line. This largely compensates for eventual uncertainties in the conversion probability. For this reason, we think that the analysis with the completely unconstrained ^{7}Be should be considered to be more reliable.

Recently, in [37] it has also been pointed out that a generic unparticle scenario will generate contact interactions between the particle operators. This contact term would generate a scattering amplitude similar to those in Eq. (8), but with $d = 2$ and $\mathcal{F}^2 = 1$.[12] Assuming that this term is dominant (and thus any interference term is negligible), the $\nu - e$ cross section is thus similar to those in Eq. (10) but with

$$\lambda_a^{\mathrm{cont}} = \left[\sum_b (\lambda_{e\nu}^{ab})^2\right]^{1/2}, \tag{28}$$

where $\lambda_{e\nu}^{ab}$ are the contact term couplings for the $\nu_a e \to \nu_b e$ scattering. The equivalent limit on $\lambda_\nu^{\mathrm{cont}}$ for $\Lambda_\mathcal{U} = 1$ TeV is $\lambda^{\mathrm{cont}} \leq 3.5$ (1.4) in the hypothesis that ^{7}Be neutrino flux is unconstrained (constrained). We do not perform a combined analysis with λ_ν and $\lambda_\nu^{\mathrm{cont}}$ unconstrained. However, since we see that the limit on is $\lambda_\nu^{\mathrm{cont}}$ in generally much weaker than those obtained for $d < 2$, if the two coupling constants were of the same magnitude, the contribution to the cross section due to the noncontact term would be dominant. In this hypothesis, the limits on λ_ν in Fig. 3 can be safely assumed.

[12]We thank B. Grinstein for pointing us to this fact.

VI. CONCLUSIONS

In this paper we have analyzed the first Borexino data release to constrain the neutrino magnetic moment and the coupling of neutrino and electrons with an hypothetical unparticle sector. The analysis is performed analyzing the spectrum of the recoil electron energy. Since the leading contribution to this spectrum comes from the monoenergetic solar ^{7}Be neutrinos, the shape of the spectrum is almost independent from the energy dependence of the oscillation probability. The other contribution to the spectral shape is due to the internal background of the detector.

We have performed a χ^2 fit assuming unconstrained solar fluxes (except for the pp and pep, which, however, give a negligible contribution) and the internal backgrounds. In the absence of nonstandard effects, our results are in good agreement with those obtained by the Borexino collaboration.

An upper limit on the neutrino magnetic moment is found: $\mu_\nu \leq 0.85 \times 10^{-10} \mu_B$. Although this is not the strongest limit in the literature, we stress that the magnetic moment measured by Borexino is a linear combination of the magnetic moments of the different neutrino flavors. Within a reasonable assumption on the oscillation probability, this limit translates into an upper one for the (much more unconstrained) μ_τ.

In the same way, we have obtained limits on the couplings with the unparticle sector. The results are summarized in Table I. In this case the limits are stronger than those obtained in the literature [19]. Furthermore, in this case the coupling constant is actually a linear combination of the couplings of neutrinos with different flavors. In this way we have obtained upper bounds on the still unknown parameters λ_μ and λ_τ. We want here to stress the fact that this limit strictly applies if *only* scalar and contact unparticle operators are present. If other operators are included in the analysis the bounds would be relaxed. A more complete analysis with further unparticle operators is deserved..

Finally, we are confident that in future Borexino will improve these limits. Since the effect of nonstandard interactions is partly hidden by the internal contaminants, a reduction or at least a better knowledge of these backgrounds would be of great help. With at least one year of data taking, using the seasonal variations of the solar neutrino flux due to the orbital eccentricity (about 3% in one year) Borexino will be able to disentangle the contribution to the spectrum coming from the ^{7}Be neutrinos to

that due to the (if constant) background. Moreover, a substantial reduction of systematics and a dramatic increase in the statistics is also expected.

ACKNOWLEDGMENTS

We are grateful to A. Ianni for fruitful discussions and suggestions and for the careful reading of the manuscript. We also thank G. Ranucci, T. Schwetz, J. W. F. Valle, and B. Grinstein for discussions. One of us (M. P.) would like to thank the organizers of PASC in Sesimbra where part of this work has been done. The work of D. M. is supported in part by the Italian ''Istituto Nazionale di Fisica Nucleare'' (INFN) and by the ''Ministero dell'Istruzione, Università e Ricerca'' (MIUR) through the ''Astroparticle Physics'' research project. J. P. is grateful to the University of Lecce for hospitality.

[1] T. Schwetz, in *Proceedings of the 9th International Workshop on Neutrino Factories, Superbeams, and Betabeams, Okayama, Japan, 2007*, AIP Conf. Proc. 981 (AIP, New York, 2008) p. 8.
[2] J. Shirai *et al.* (KamLAND Collaboration), Nucl. Phys. B, Proc. Suppl. **168**, 77 (2007).
[3] M. Picariello *et al.*, J. High Energy Phys. 11 (2007) 055.
[4] G. Alimonti *et al.* (Borexino Collaboration), Phys. Lett. B **658**, 101 (2008).
[5] J. N. Bahcall, A. M. Serenelli, and S. Basu, Astrophys. J. Suppl. Ser. **165**, 400 (2006).
[6] P. Vogel and J. Engel, Phys. Rev. D **39**, 3378 (1989).
[7] H. T. Wong *et al.* (TEXONO Collaboration), Phys. Rev. D **75**, 012001 (2007).
[8] A. G. Beda *et al.*, arXiv:0705.4576.
[9] A. Ianni, D. Montanino, and G. Scioscia, Eur. Phys. J. C **8**, 609 (1999).
[10] W.-M. Yao *et al.* (Particle Data Group), J. Phys. G **33**, 1 (2006).
[11] M. Raidal *et al.*, arXiv:0801.1826.
[12] A. M. Mourao, J. Pulido, and J. P. Ralston, Phys. Lett. B **285**, 364 (1992); **288**, 421 (1992).
[13] J. Pulido and A. M. Mourao, Phys. Rev. D **57**, 1794 (1998).
[14] J. F. Beacom and P. Vogel, Phys. Rev. Lett. **83**, 5222 (1999).
[15] W. Grimus *et al.*, Nucl. Phys. **B648**, 376 (2003).
[16] D. W. Liu *et al.* (SuperKamiokande Collaboration), Phys. Rev. Lett. **93**, 021802 (2004).
[17] H. O. Back *et al.*, Phys. Lett. B **563**, 35 (2003).
[18] H. Georgi, Phys. Rev. Lett. **98**, 221601 (2007).
[19] A. B. Balantekin and K. O. Ozansoy, Phys. Rev. D **76**, 095014 (2007).
[20] G. t'Hooft, Phys. Lett. **37B**, 195 (1971).
[21] J. N. Bahcall, M. Kamionkowski, and A. Sirlin, Phys. Rev. D **51**, 6146 (1995).
[22] J. Barranco *et al.*, arXiv:0711.0698.
[23] A. Mirizzi, D. Montanino, and P. D. Serpico, Phys. Rev. D **76**, 053007 (2007).
[24] G. G. Raffelt, Phys. Rev. Lett. **81**, 4020 (1998).
[25] L. B. Auerbach *et al.* (LSND Collaboration), Phys. Rev. D **63**, 112001 (2001).
[26] R. Schwienhorst *et al.* (DONUT Collaboration), Phys. Lett. B **513**, 23 (2001).
[27] K. Cheung, W. Y. Keung, and T. C. Yuan, Phys. Rev. Lett. **99**, 051803 (2007); Phys. Rev. D **76**, 055003 (2007).
[28] S. Zhou, Phys. Lett. B **659**, 336 (2008).
[29] G. Alimonti *et al.* (Borexino Collaboration), Astropart. Phys. **16**, 205 (2002).
[30] E. J. Konopinsky and G. E. Uhlenbeck, Phys. Rev. **60**, 308 (1941).
[31] J. N. Bahcall, Phys. Rev. D **49**, 3923 (1994).
[32] P. C. de Holanda, W. Liao, and A. Y. Smirnov, Nucl. Phys. **B702**, 307 (2004).
[33] J. Pulido, Phys. Rep. **211**, 167 (1992).
[34] A. Strumia and F. Vissani, arXiv:hep-ph/0606054.
[35] Z. Berezhiani, R. S. Raghavan, and A. Rossi, Nucl. Phys. **B638**, 62 (2002).
[36] M. C. Gonzalez-Garcia, P. C. de Holanda, and R. Zukanovich Funchal, arXiv:0803.1180.
[37] B. Grinstein, K. Intriligator, and I. Z. Rothstein, Phys. Lett. B **662**, 367 (2008).